Improved subsalt tomography using RTM surface offset gathers

Zhiping Yang, Shouting Huang, Rui Yan, CGG*

Summary

Subsalt tomography, a critical step in subsalt imaging, is often a challenging task because of the poor illumination and strong noise contamination of the subsalt region. Adding to the difficulty of this process is the lack of good pre-stack common image gathers (CIGs) to extract reliable gather curvature. To overcome this, a common practice is to produce reverse time migration (RTM) angle gathers and perform a tomographic velocity update on them. However, there are two drawbacks associated with standard common-shot RTM angle gathers: (1) subsalt events on angle gathers are usually present for a narrow range of incident angles (i.e., $<30^o$), and (2) in the presence of migration velocity error, residual curvatures of subsalt events are often degraded due to interference caused by wavefronts propagating from different surface offsets. The degradation resulting from offset interference increases with the offset of the input data.

On the other hand, RTM surface offset gathers (SOGs) often contain subsalt events spanning the entire offset range (i.e., longer usable curvatures for tomography). RTM SOGs also have more reliable residual curvatures because each offset and azimuth group is migrated independently and does not interfere with the neighboring ones. RTM SOGs are more beneficial for full azimuth (FAZ) and ultra-long offset data.

Introduction

As marine seismic acquisition methods for subsalt exploration progress from 2D to 3D and from narrow azimuth (NAZ) to wide azimuth (WAZ) and full azimuth (FAZ) with ultra-long offsets (e.g., up to 18 km), we obtain an everincreasing volume of data designed to illuminate difficult subsalt targets. The abundant measurements not only improve the signal-to-noise ratio of subsalt reflections, but they also provide rich offset and azimuthal information for subsalt velocity analysis. The classic migration velocity analysis approach consists of three steps: (1) generate offset-domain CIGs or SOGs from a ray-based Kirchhoff migration, (2) pick residual curvatures from the SOGs, and (3) update the velocity using a ray-based tomographic inversion (Guillaume et al., 2008). For subsalt regions, the abovementioned Kirchhoff-based velocity analysis is problematic and rarely used. Problems arise from its poor image quality caused by the instability and multi-pathing problem of tracing rays through salt. In practice, shot-profile RTM, a 2-way wave-equation migration method, is the preferred migration technique for subsalt imaging and velocity updating in areas such as the Gulf of Mexico.

Constructing SOGs from RTM is a difficult exercise. A shot-profile or common-shot RTM is more conducive to construct angle-domain CIGs (ADCIGs) or angle gathers. Many methods have been proposed for computing RTM angle gathers. Xu et al. (2011) used a direct wavefront decomposition approach, Dickens et al. (2011) computed wavefronts from Poynting vector estimation, and Sava et al. (2011) constructed angle gathers from Tau-P transformation of subsurface offset gathers.

Because of the familarity with using SOGs for velocity analysis and imaging, many attempts have been made to construct SOGs from RTM. Two notable methods were proposed by Giboli et al. (2012) and Etgen (2012). Giboli et al. (2012) applied the migration of attribute proposed by Bleistein (1987) to common shot RTM and surface offset. Surface offset is recovered after migration by dividing RTM image of data multiplied by offset by RTM image of standard data. The recovered surface attribute then serves as a 3D map to redistribute the common-shot image to generate SOGs. Etgen (2012) proposed a 3D wave-equation Kirchhoff migration. He suggested that, instead of using ray tracing for travel-time table computation, a wave extrapolation method is used for the computation. Then, the input data are sorted to maximize the use of local travel time information. This approach enables a stable penetration of complex salt geometry, and the migration output can be readily sorted into SOGs.

We present an alternative method for generating SOGs that uses a common-offset RTM scheme. First, on the receiver side, we split the recorded data into offset groups and back-propagate the wavefield for each group separately. Second, on the shot side, which is an impulse from the shot location, we propagate the source wavefield in its entirety. Finally, we form SOGs based on the common imaging outputs between the split receiver wavefields and the source wavefield. Our method is computationally more expensive than the attribute coding method but less expensive than the wave-equation Kirchhoff method. The attribute coding method relies on the stability of dividing two stacked images, which could suffer from the energy leakage from neighboring offsets. Whereas the wave-equation Kirchhoff method involves approximations in bundling neighboring traces for travel time information unless every single trace is migrated separately. Our method does not rely on these approximations, and the resulting SOGs are more accurate. We examine the quality between SOGs and RTM angle gathers as well as the resulting tomographic updates.

DOI http://dx.doi.org/10.1190/segam2015-5848366.1

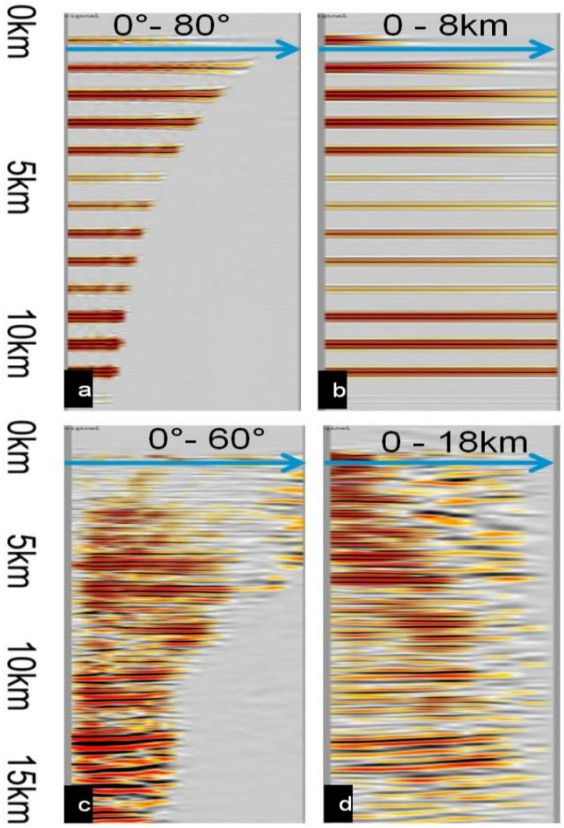

Figure 1: Comparison of reverse time migration (RTM) angle gathers and surface offset gathers (SOGs). (a) and (b) are synthetic examples with a maximum offset of 8 km. (c) and (d) are real data examples with a maximum offset of 18 km.

Maximum angle vs. offset in depth

To compare the characteristics of RTM angle gathers and SOGs, we started with a simple 1.5D synthetic model that had a constant velocity, ten evenly spaced reflectors, and a surface offset ranging from 0 to 8 km. The resulting RTM angle gather showed that the maximum incident angle gradually decreased with depth and eventually shrank to less than 20º for the bottom reflector (Figure 1a). The decreasing maximum angle indicated the propagation angle was moving closer to vertical. In the Gulf of Mexico, the maximum angle of a subsalt event is normally less than 30º. In contrast, the SOGs (Figure 1b) contained uniform reflectors spanning the entire offset range from top to bottom. We observed a similar trend in real FAZ data from the Gulf of Mexico (Figures 1c and 1d). For reflectors between 10 to 15 km, roughly half of the angle gather was empty, while the SOGs had usable information for the entire gather. In theory, both gathers contain the same information and can be uniquely mapped from one to the other. However, in practice, the residual curvature picked from offset gathers tends to be more reliable due to ample sampling along the offset axis.

Gather curvature

Montel and Lambaré (2011) investigated the curvature difference between common-offset gathers (i.e., SOGs) and common-shot gathers (i.e., angle gathers) and provided an asymptotic formula for gather curvatures at the high-frequency limit. Their study showed that due to the specularity condition difference, the curvature in angle gathers may differ very signicantly for the same migration velocity error.

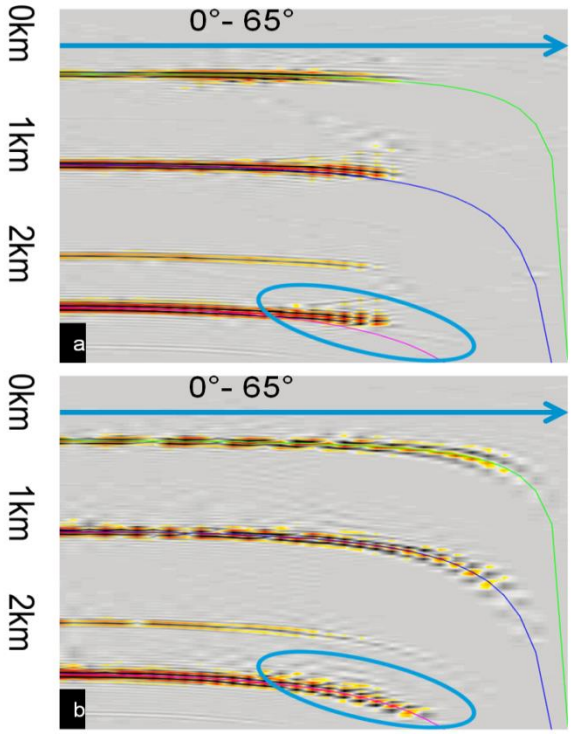

Figure 2: Curvature comparison of angle gather generated by (a) common-shot migration and (b) common-offset migration.

To demonstrate the curvature difference between angle gathers generated by common-shot and common-offset migrations, we used another simple 1.5D synthetic model. This model consisted of one constant velocity and three flat reflectors. For a fair comparison, all images were presented in the angle domain. Figure 2a shows an angle gather generated by common-shot migration with wavefront decomposition (Xu et al., 2011); Figure 2b shows the angle gather from common-offset migration, which was obtained by splitting recorded wavefields into offset groups (same as for SOG). We migrated each offset group separately and

DOI http://dx.doi.org/10.1190/segam2015-5848366.1

output an angle gather for each offset group. Then, we stacked all the angle gathers per common depth point (CDP) per angle to obtain the final angle gather. Both migrations used the same velocity model, which was 10% too fast. The solid curves indicate the common-offset theoretical curvatures at different depths. The curvatures of standard common-shot angle gathers deviated from the common-offset theoretical prediction at large angles, while curvatures of angle gathers produced by splitting recorded wavefields matched well with the common-offset theoretical prediction at all angles.

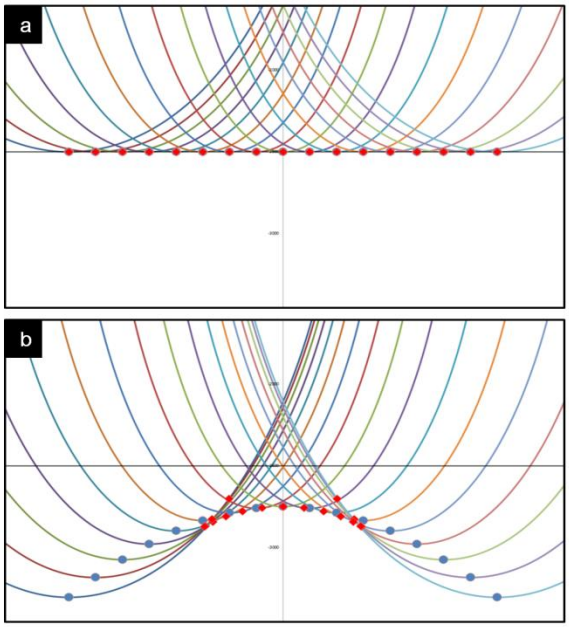

Figure 3: High-frequency limit study of the contributions to the final image from different offsets. (a) Migrated at correct velocity. (b) Migrated at +10% velocity error. Stationary points under common-offset specularity condition is indicated by the blue dots and under common-shot specularity condition is indicated by the red diamonds.

To understand the destructive interference of different offsets under the wrong migration model, we conducted a theoretical high-frequency limit study (Figure 3). This can be viewed as a common-shot migration with receivers at separated surface offset locations and a single shot at the surface in the middle. With a constant velocity 1.5D model, the travel time for each offset can be expressed as:

$$t_a = \frac{\sqrt{4d^2+h^2}}{v_a}, \qquad (1)$$

where v_a is the velocity, d is the reflector depth, and h is the surface offset.

The contribution from each offset to the final stack image is color-coded (Figures 3a and 3b). The equations for these curves are

$$\sqrt{(x-x_s)^2+(y-y_s)^2}+\sqrt{(x-x_r)^2+(y-y_r)^2}=v_m t_a, \qquad (2)$$

where x_s, y_s and x_r, y_r are source and receiver coordinates, respectively; and v_m is the migration velocity.

When migrated at the correct velocity (Figure 3a), stationary points (both common-shot and common-offset) for all offsets were preserved for common-shot migration. However, when the migration velocity was wrong (Figure 3b), common-offset stationary points from all offsets were no longer preserved for common-shot migration. Depending on the amount of error in the migration velocity, only a few near offsets can survive the destructive interference from neighboring offsets, while all the common-offset stationary points of far offsets stacked destructively. Thus, if the migration velocity is wrong, the part from each curve that contributes to the offset gather differs between common-offset and common-shot migration. When the migration velocity error is large, the common-shot stationary points at far offset tend to cluster together or even becomes unstable, effectively destroying the curvature information contained in those offsets.

On the other hand, with our RTM SOG method, which separates the recorded wavefields by offsets and migrates each of them separately, the stationary point of each offset was preserved because it did not suffer from destructive interference caused by neighboring offsets. In essence, regardless of the migration velocity error, RTM SOGs contained more reliable curvature information, particularly from the contributions of large offsets. For this exact reason, the far angle by the common-shot migration lost most of its energy (Figure 2a) under the wrong migration model, while the far angle by the common-offset migration survived (Figure 2b).

Application of RTM SOG on FAZ and ultra-long offset data

We generated both RTM angle gathers and SOGs using FAZ data from the Gulf of Mexico (full azimuth to 10 km and ultra-long offset up to 18 km). We then compared the tomographic results from common-shot angle gather vs. common-offset SOGs. For a one-to-one comparison, the angle gather update was also evaluated using the RTM SOG. Figures 4a and 4b show the stack and SOGs before tomographic update, respectively; Figures 4c and 4d show the stack and SOGs after tomographic updates using RTM angle gathers; and Figures 4e and 4f show the stack and SOGs after RTM SOG tomographic update. Overall, the tomographic update using RTM SOGs produced flatter gathers and a more focused stacked image (red circle).

DOI http://dx.doi.org/10.1190/segam2015-5848366.1

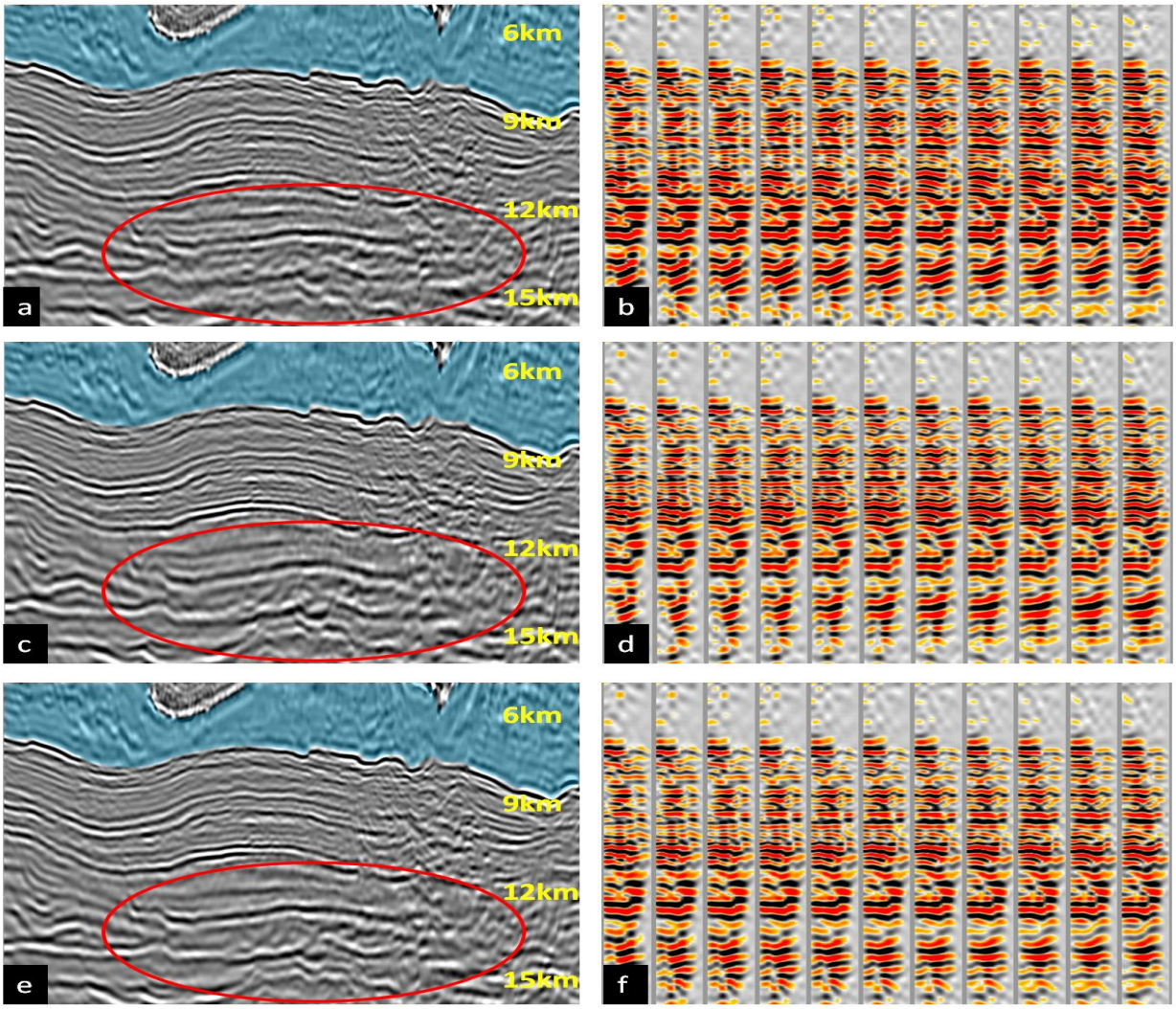

Figure 4: Stack and RTM SOGs (a, b) before subsalt tomographic update, (c, d), after angle gather tomographic update, and (e, f) after RTM SOG tomographic update, respectively.

Conclusions

We examined the differences between angle gathers from common-shot RTM and SOGs from common-offset RTM. We illustrated that RTM SOGs provide ample sampling of residual curvatures, particularly those from deep events. We also demonstrated that RTM SOGs generated from a common-offset RTM preserve longer usable residual curvatures at large offsets in the presence of migration velocity errors. Using a real FAZ and ultra-long offset data example, we verified that using RTM SOGs produces better subsalt tomographic velocity updates. In addition to its application to subsalt tomography, RTM SOGs also provide additional surface offset information that could be useful in diagnostics of alternate salt interpretations. However, a potential drawback of our method is that in complex areas, RTM SOGs may suffer from the multipath problem (Xu et al., 2001). Also, our method involves many additional propagations of the receiver wavefields and thus it is computationally expensive. Using our method to generate RTM SOGs for an imaging project requires ready access to high performance computing.

Acknowledgements

We thank Fred Li, Tony Huang, and Shuo Ji for their inspiring discussions and comments. We also thank CGG for the permission to publish this work.

DOI http://dx.doi.org/10.1190/segam2015-5848366.1

EDITED REFERENCES

Note: This reference list is a copyedited version of the reference list submitted by the author. Reference lists for the 2015 SEG Technical Program Expanded Abstracts have been copyedited so that references provided with the online metadata for each paper will achieve a high degree of linking to cited sources that appear on the Web.

REFERENCES

Bleistein, N., 1987, On the imaging of reflectors in the earth: Geophysics, **52**, 931–942, http://dx.doi.org/10.1190/1.1442363.

Dickens, T. A., and G. A. Winbow, 2011, RTM angle gathers using Poynting vectors: 81st Annual International Meeting, SEG, Expanded Abstracts, 3109–3113.

Etgen, J. T., 2012, 3D wave equation Kirchhoff migration: 82nd Annual International Meeting, SEG, Expanded Abstracts, doi:10.1190/segam2012-0755.1.

Giboli, M., R. Baina, L. Nicoletis, and B. Duquet, 2012, Reverse time migration surface offset gathers, Part 1: A new method to produce 'classical' common image gathers: 82nd Annual International Meeting, SEG, Expanded Abstracts, doi:10.1190/segam2012-1007.1.

Guillaume, P., G. Lambaré, O. Leblanc, P. Mitouard, J. Le Moigne, J.-P. Montel, T. Prescott, R. Siliqi, N. Vidal, X. Zhang, and S. Zimine, 2008, Kinematic invariants: An efficient and flexible approach for velocity model building: 78th Annual International Meeting, SEG, Expanded Abstracts, 3687–3692.

Montel, J.-P., and G. Lambaré, 2011, RTM and Kirchhoff angle domain common-image gathers for migration velocity analysis: 81st Annual International Meeting, SEG, Expanded Abstracts, 3120–3124.

Sava, P., and I. Vlad, 2011, Wide-azimuth angle gathers for wave-equation migration: Geophysics, **76**, no. 3, S131–S141, http://dx.doi.org/10.1190/1.3560519.

Xu, S., H. Chauris, G. Lambaré, and M. Noble, 2001, Common-angle migration: A strategy for imaging complex media: Geophysics, **66**, 1877–1894, http://dx.doi.org/10.1190/1.1487131.

Xu, S., Y. Zhang, and B. Tang, 2011, 3D angle gathers from reverse time migration: Geophysics, **76**, no. 2, S77–S92, http://dx.doi.org/10.1190/1.3536527.

DOI http://dx.doi.org/10.1190/segam2015-5848366.1